

Open-loop vs. Closed-loop identification of Box-Jenkins systems in a Least Costly Identification context

Xavier Bombois, Brian D.O. Anderson and Gérard Scorletti

Abstract—In this paper, we compare open-loop and closed-loop prediction error identification. In particular, we determine whether open-loop or closed-loop identification is optimal in the least costly identification experiment design framework. The least costly experiment design framework is a new framework for optimal experiment design where the objective is to determine the cheapest identification while ensuring that the accuracy of the identified model is above some nominated threshold. A second contribution of this paper is to develop a control design algorithm which ensures that the designed controller both ensures sufficient closed-loop performance with the true system, but also ensures that a model identified via closed-loop identification on the designed loop has high accuracy.

I. INTRODUCTION

In an earlier contribution [3], we compared the open-loop and closed-loop identification of a Box-Jenkins (BJ) true system:

$$y(t) = G(z, \rho_0)u(t) + \overbrace{H(z, \eta_0)}^{v(t)}e(t) \text{ for some } \theta_0 = \begin{pmatrix} \rho_0 \\ \eta_0 \end{pmatrix} \quad (1)$$

where $e(t)$ is a white noise of variance σ_e^2 and $G(z, \rho_0)$ and $H(z, \eta_0)$ are independently parametrized rational transfer functions. The open-loop and closed-loop identifications were supposed to be performed in a full-order model structure (i.e. $\mathcal{S} \in \mathcal{M}$) using the prediction error framework [13]. In particular, we looked at the covariance matrix P_ρ of the identified parameter vector $\hat{\rho}_N$ and at the covariance matrix P_η of the identified parameter vector $\hat{\eta}_N$ and we determined ordering relations between these matrices when obtained both through open-loop and through closed-loop identifications. Roughly speaking, the main contribution of [3] was to determine under which conditions the accuracy P_ρ^{-1} of $\hat{\rho}_N$ is larger in closed-loop identification than in open-loop identification; the accuracy P_η^{-1} of $\hat{\eta}_N$ is always smaller in closed-loop identification than in open-loop identification.

X. Bombois is with the Delft Center for Systems and Control, Delft University of Technology, The Netherlands, X.J.A.Bombois@tudelft.nl

Brian D.O. Anderson is with the Australian National University and National ICT Australia. Brian.Anderson@anu.edu.au. National ICT Australia is funded by the Australian Government's Department of Communications, Information Technology and the Arts and the Australian Research Council through *Backing Australia's Ability* and the ICT Centre of Excellence program.

G. Scorletti is with GREYC Equipe AUTO, Caen, France gerard.scorletti@greyc.ensicaen.fr

In the present paper, we continue the analysis begun in [3]. The contributions of this paper are twofold. First, we determine the consequences of the results [3] for optimal experiment design. This is a very common subject in the system identification literature. In [14], [1] and in Chapter 13 of [13], the authors address the problem of knowing whether open-loop or closed-loop identification is optimal when we want to maximize a measure of the accuracy of the identified model under some power constraints for the input and/or the output signals. Other typical contributions in this literature are [9], [10].

However, in the present paper, we address the question of knowing whether open-loop or closed-loop identification is optimal when we consider another appealing framework for optimal experiment design i.e. the least costly identification experiment design framework (LCID). The LCID framework is a new framework for optimal experiment design where the objective is to determine the identification experiment with the smallest economical cost while ensuring that the accuracy of the identified model $G(z, \hat{\rho}_N)$ remains above some nominated threshold i.e. $P_\rho^{-1} \geq R_{adm}$ [5], [12], [2], [6]. This threshold is generally determined in such a way that a robust controller for the true system can only be designed with the identified model if the accuracy of the identified model is above this threshold. We show in the sequel that, when the cost of the identification is defined by the perturbation induced by the excitation signal on the output signal, closed-loop identification is optimal (i.e., under the same constraint $P_\rho^{-1} \geq R_{adm}$, a closed-loop identification always induces a smaller perturbation on the output signal than an open-loop identification). When the cost of the identification is defined by its duration, then open-loop identification, perhaps surprisingly, turns out to be optimal.

The second contribution of this paper consists of analyzing qualitatively and quantitatively the role of the controller C_{id} present in the loop for closed-loop identification. The controller plays indeed an important role in the achieved accuracy of the identified models. More particularly, we show that, if the controller C_{id} implies a high correlation between the identified parameter vectors $\hat{\rho}_N$ and $\hat{\eta}_N$, the achieved accuracies P_ρ^{-1} for $\hat{\rho}_N$ and P_η^{-1} for $\hat{\eta}_N$ are lessened. Indeed, we will show that the existence of this correlation implies that the contribution of the noise to the accuracy of $\hat{\rho}_N$ and $\hat{\eta}_N$ is not as high as it could be. This observation evidences the benefit of forcing this

correlation to be as small as possible, by appropriately choosing the controller in the loop. We therefore develop a novel control design algorithm where the objective is not only to ensure that the designed closed loop $[C_{id} G_0]$ has satisfactory closed-loop H_∞ performance (for e.g. tracking and disturbance rejection), but also that, if we need to perform a closed-loop identification within this loop, this closed-loop identification will result in the smallest possible correlation between $\hat{\rho}_N$ and $\hat{\eta}_N$ (and thus with high accuracy for $\hat{\eta}_N$ and $\hat{\rho}_N$).

To our knowledge, it is the first time that these two objectives have been tackled together in a control design algorithm and it is the first time that an objective relating the correlation between $\hat{\rho}_N$ and $\hat{\eta}_N$ has been used to increase the value of the accuracy P_ρ^{-1} of $\hat{\rho}_N$ and the accuracy P_η^{-1} of $\hat{\eta}_N$ for closed-loop identification. Generally, in the system identification literature [9], [10], [11], [14], the objective is to determine the optimal controller C_{id} for a closed-loop identification without constraining the closed-loop control performance. For some specific objectives, the optimal controller for closed-loop identification appears to be the minimum variance controller [9], [14] which has (relatively) good closed-loop control performance. However, if we determine the optimal controller C_{id} for other identification objectives using the methodologies developed in [11], it is not at all guaranteed that this controller will have satisfactory closed-loop control performance. Moreover, the controller designed using these methods is only optimal for the specific closed-loop identification objectives for which it has been designed. It is not at all guaranteed that it is optimal for other objectives. As opposed to this, our approach pertaining to the values of the matrices P_ρ^{-1} and P_η^{-1} seems a reasonable objective in all situations (i.e. for all closed-loop identification objectives)

II. VARIANCE ASPECTS FOR BOX-JENKINS SYSTEMS

As mentioned in the introduction, we consider the identification of a stable linear time-invariant single input single output Box-Jenkins system (1) with a model structure \mathcal{M} that is able to represent the true system i.e. $\mathcal{S} \in \mathcal{M}$.

In this paper, we will consider both open-loop and closed-loop identification [13]. In open-loop identification, the system is excited by applying a quasi-stationary input signal $u(t) = u_{OL}(t)$ to (1) and, in closed-loop identification, by the application of a quasi-stationary signal $r(t)$ [13] such that:

$$\begin{aligned} y_{CL}(t) &= y_e(t) + y_r(t) = S_{id}H(z, \eta_0)e(t) + G_0S_{id}r(t) \quad (2) \\ u_{CL}(t) &= u_e(t) + u_r(t) = -C_{id}S_{id}H(z, \eta_0)e(t) + S_{id}r(t) \quad (3) \end{aligned}$$

with C_{id} the controller present in the (forward part of the) loop and $S_{id} = (1 + C_{id}G(z, \rho_0))^{-1}$. In both situations, a model $\hat{G}(z) = G(z, \hat{\rho}_N)$, $\hat{H}(z) = H(z, \hat{\eta}_N)$ of the true system is obtained by collecting N input

and output data $\{u(t), y(t), t = 1, \dots, N\}$. Using these data, the estimated parameter vector $\hat{\theta}_N = (\hat{\rho}_N^T \hat{\eta}_N^T)^T$ is given by: $\hat{\theta}_N \triangleq \arg \min_{\theta} \frac{1}{N} \sum_{t=1}^N \epsilon^2(t, \theta)$ with $\epsilon(t, \theta) \triangleq H(z, \eta)^{-1} (y(t) - G(z, \rho)u(t))$. The identified parameter vector $\hat{\theta}_N$ is (asymptotically) normally distributed around the true parameter vector θ_0 , i.e. $\hat{\theta}_N \sim \mathcal{N}(\theta_0, P_\theta)$ with P_θ a strictly positive definite matrix given by [13][Chapter 9]:

$$P_\theta = \frac{\sigma_e^2}{N} \left(\bar{E} \left(\psi(t, \theta_0) \psi(t, \theta_0)^T \right) \right)^{-1} \text{ with } \psi(t, \theta) = -\frac{\partial \epsilon(t, \theta)}{\partial \theta}. \quad (4)$$

If we now partition the covariance matrix P_θ according to the partition of the parameter vector θ_0 in (1) i.e. $P_\theta = \begin{pmatrix} P_\rho & P_{\rho\eta} \\ P_{\rho\eta}^T & P_\eta \end{pmatrix}$, we obtain a distinct distribution for each of the identified parameter vectors $\hat{\rho}_N$ and $\hat{\eta}_N$:

$$\hat{\rho}_N \sim \mathcal{N}(\rho_0, P_\rho) \quad \hat{\eta}_N \sim \mathcal{N}(\eta_0, P_\eta). \quad (5)$$

Based on these expressions, we can deduce parametric uncertainty regions for the unknown $G(z, \rho_0)$ and the unknown $H(z, \eta_0)$ centered at the identified model $G(z, \hat{\rho}_N)$ and $H(z, \hat{\eta}_N)$ (see e.g. [4]). The sizes of these uncertainty regions are determined by the covariance matrices P_ρ and P_η . Using Gauss' approximation formula [13], the variances at $z = e^{j\omega}$ of the identified plant model $G(z, \hat{\rho}_N)$ and the identified noise model $H(z, \hat{\eta}_N)$ are function of P_η and P_ρ , respectively:

$$\begin{aligned} \text{var}(G(e^{j\omega}, \hat{\rho}_N)) &= \Lambda_\rho^*(e^{j\omega}, \rho_0) P_\rho \Lambda_\rho(e^{j\omega}, \rho_0) \\ \text{var}(H(e^{j\omega}, \hat{\eta}_N)) &= \Lambda_\eta^*(e^{j\omega}, \eta_0) P_\eta \Lambda_\eta(e^{j\omega}, \eta_0) \quad (6) \end{aligned}$$

where $\Lambda_\rho(z, \rho) = \frac{\partial G(z, \rho)}{\partial \rho}$ and $\Lambda_\eta(z, \eta) = \frac{\partial H(z, \eta)}{\partial \eta}$. The covariance matrices P_ρ and P_η are thus perfect tools to compare the accuracy of an identification experiment under different experimental conditions, i.e., in particular, in order to compare the variances obtained by open-loop and closed-loop identification. For this purpose, it is important to derive appropriate expressions for P_ρ and P_η for both identification conditions. To do this, we first particularize $\psi(t, \theta_0)$ in (4) to the BJ-case. In closed-loop identification, this becomes:

$$\psi(t, \theta_0) = \begin{pmatrix} \frac{S_{id}}{H(z, \eta_0)} \Lambda_\rho(z, \rho_0) \\ 0 \end{pmatrix} r(t) + \begin{pmatrix} -C_{id} S_{id} \Lambda_\rho(z, \rho_0) \\ \frac{\Lambda_\eta(z, \eta_0)}{H(z, \eta_0)} \end{pmatrix} e(t) \quad (7)$$

For open-loop identification, $\psi(t, \theta_0)$ reduces to:

$$\psi(t, \theta_0) = \begin{pmatrix} \frac{\Lambda_\rho(z, \rho_0)}{H(z, \eta_0)} \\ 0 \end{pmatrix} u(t) + \begin{pmatrix} 0 \\ \frac{\Lambda_\eta(z, \eta_0)}{H(z, \eta_0)} \end{pmatrix} e(t) \quad (8)$$

Based on these particular expressions for $\psi(t, \theta_0)$, we can deduce the expression for P_θ in open-loop and closed-loop identifications using the definition (4):

$$P_{\theta, OL}^{-1} = \begin{pmatrix} \Xi_{OL} & 0 \\ 0 & 0 \end{pmatrix} + \begin{pmatrix} 0 & 0 \\ 0 & R_{v,22} \end{pmatrix} \quad (9)$$

$$P_{\theta,CL}^{-1} = \begin{pmatrix} \Xi_{CL} & 0 \\ 0 & 0 \end{pmatrix} + \begin{pmatrix} R_{v,11} & R_{v,12} \\ R_{v,12}^T & R_{v,22} \end{pmatrix}. \quad (10)$$

with

$$\Xi_{OL} = \frac{N}{\sigma_e^2} \mathcal{I} \left(\frac{\Lambda_\rho(z, \rho_0)}{H(z, \eta_0)}, \Phi_u(\omega) \right) \quad (11)$$

$$\Xi_{CL} = \frac{N}{\sigma_e^2} \mathcal{I} \left(S_{id} \frac{\Lambda_\rho(z, \rho_0)}{H(z, \eta_0)}, \Phi_r(\omega) \right) \quad (12)$$

$$R_{v,11} = N \mathcal{I}(C_{id} S_{id} \Lambda_\rho(z, \rho_0), 1)$$

$$R_{v,12} = N \frac{1}{2\pi} \int_{-\pi}^{\pi} \frac{-C_{id} S_{id} \Lambda_\rho(e^{j\omega}, \rho_0) \Lambda_\eta^*(e^{j\omega}, \eta_0)}{H^*(z, \eta_0)} d\omega$$

$$R_{v,22} = N \mathcal{I} \left(\frac{\Lambda_\eta(z, \eta_0)}{H(z, \eta_0)}, 1 \right) \text{ and}$$

$$\mathcal{I}(V(z), \Phi(\omega)) \triangleq \frac{1}{2\pi} \int_{-\pi}^{\pi} V(e^{j\omega}) V(e^{j\omega})^* \Phi(\omega) d\omega$$

It is important for the sequel to note that the noise contribution to the inverse covariance matrix $P_{\theta,CL}^{-1}$ in (10) is, in almost all cases, strictly positive-definite:

$$\begin{pmatrix} R_{v,11} & R_{v,12} \\ R_{v,12}^T & R_{v,22} \end{pmatrix} > 0 \quad (13)$$

Indeed, provided the parametrization in (1) is such that $\rho_0 \rightarrow G(z, \rho_0)$ and $\eta_0 \rightarrow G(z, \eta_0)$ are one-to-one mappings (as is reasonable), it is very unlikely that one element of the vector defining the noise contribution in (7) can be written as a linear combination of the other elements. Consequently, in the sequel, it will be always assumed that (13) holds. It is also important to note that the matrix $R_{v,12}$ is generally non-zero: there is thus correlation between $\hat{\rho}_N$ and $\hat{\eta}_N$ when those are identified in closed loop, unlike when they are identified in open loop (see (9)).

Given the expressions (9)-(10) for P_θ^{-1} and the partition of P_θ above (5), we can now deduce expressions for (the inverse of) P_ρ and P_η via a straightforward application of the matrix inversion formula (see e.g. [18][page 14]):

$$P_{\rho,OL}^{-1} = \Xi_{OL} \quad (14)$$

$$P_{\rho,CL}^{-1} = \Xi_{CL} + R_{v,11} - R_{v,12} R_{v,22}^{-1} R_{v,12}^T \quad (15)$$

$$P_{\eta,OL}^{-1} = R_{v,22} \quad (16)$$

$$P_{\eta,CL}^{-1} = R_{v,22} - R_{v,12}^T (\Xi_{CL} + R_{v,11})^{-1} R_{v,12} \quad (17)$$

Note that (15) can also be found in [8]. As evidenced in our earlier paper [3], these formulae give interesting insights about the accuracy of $\hat{\rho}_N$ and $\hat{\eta}_N$ when identified in open loop or in closed loop. The following proposition summarizes the main observations of [3]. In this proposition, two different conditions on the input power spectrum will be introduced to allow comparison of open loop and closed loop identification. The spectrum equality condition of item

2 in Proposition 1 amounts to requiring that the power spectrum of the plant input is the same in the open and closed-loop cases, while the spectrum equality condition in item 3 requires that the part of the plant input spectrum independent of the output noise to be the same in the open and closed-loop cases. The motivation for these conditions will become evident when, in Section IV, we will discuss optimal experiment design.

Proposition 1 ([3]): Consider two identification experiments on the same BJ true system (1) and of the same duration N : one in open loop with input spectrum $\Phi_u^{OL}(\omega)$ and one in closed loop with excitation spectrum $\Phi_r(\omega)$ and a controller C_{id} in the loop. Assume further that $R_{v,12} \neq 0$ and that (13) holds. Then:

- 1) independently of $\Phi_u^{OL}(\omega)$, $\Phi_r(\omega)$ and C_{id} , we have that $P_{\eta,OL} \leq P_{\eta,CL}$ and thus that $\text{var}(\hat{H}_{OL}(e^{j\omega})) \leq \text{var}(\hat{H}_{CL}(e^{j\omega})) \forall \omega$
- 2) independently of C_{id} , if $\Phi_r(\omega)$ is chosen such that $\Phi_u^{CL}(\omega) = \Phi_u^{OL}(\omega) \forall \omega$, we have that $P_{\rho,OL} \leq P_{\rho,CL}$ and thus that $\text{var}(\hat{G}_{OL}(e^{j\omega})) \leq \text{var}(\hat{G}_{CL}(e^{j\omega})) \forall \omega$
- 3) independently of C_{id} , if $\Phi_r(\omega)$ is chosen such that $|S_{id}(e^{j\omega})|^2 \Phi_r(\omega) = \Phi_u^{OL}(\omega) \forall \omega$, we have that $P_{\rho,OL} > P_{\rho,CL}$ and thus that $\text{var}(\hat{G}_{OL}(e^{j\omega})) > \text{var}(\hat{G}_{CL}(e^{j\omega})) \forall \omega$. This also holds when $R_{v,12} = 0$.

Proof. Item 1 follows directly from (16)-(17). To prove Item 2, we see that, in (15), $\Xi_{CL} + R_{v,11} =$

$$\begin{aligned} &= N \mathcal{I}(\Lambda_\rho, \frac{|S_{id}(e^{j\omega})|^2 \Phi_r(\omega)}{\Phi_v(\omega)}) + \mathcal{I}(\Lambda_\rho, \frac{|C_{id} S_{id}(e^{j\omega})|^2 \Phi_v(\omega)}{\Phi_v(\omega)}) \\ &= \frac{N}{\sigma_e^2} \mathcal{I}(\frac{\Lambda_\rho}{H_0}, \Phi_u^{CL}(\omega)) \end{aligned}$$

where $\Phi_v(\omega)$ is the power spectrum of $v(t) = H_0(z)e(t) = H(z, \eta_0)e(t)$ and where the last step follows from (2). Now, since it is assumed that $\Phi_u^{CL}(\omega) = \Phi_u^{OL}(\omega) \forall \omega$, we have that $\Xi_{OL} = \Xi_{CL} + R_{v,11}$ and thus that $P_{\rho,CL}^{-1} = P_{\rho,OL}^{-1} - R_{v,12} R_{v,22}^{-1} R_{v,12}^T$. This delivers the result since $R_{v,12} R_{v,22}^{-1} R_{v,12}^T \geq 0$ by assumption. Item 3 can be proven similarly to Item 2. Indeed, when $|S_{id}(e^{j\omega})|^2 \Phi_r(\omega) = \Phi_u^{OL}(\omega) \forall \omega$, $\Xi_{OL} = \Xi_{CL}$ and thus $P_{\rho,CL}^{-1} = P_{\rho,OL}^{-1} + R_{v,11} - R_{v,12} R_{v,22}^{-1} R_{v,12}^T$. This delivers the result since $R_{v,11} - R_{v,12} R_{v,22}^{-1} R_{v,12}^T > 0$ by assumption. ■

This proposition shows that, in closed-loop identification, both the parts $u_r(t)$ and $u_e(t)$ of $u_{CL}(t)$ (see (2)) contribute to the precision $P_{\rho,CL}^{-1}$ of $\hat{\rho}_N$: the part $u_r(t)$ via Ξ_{CL} and the part $u_e(t)$ via $R_{v,11}$. However, the coupling between $\hat{\rho}_N$ and $\hat{\eta}_N$ somehow decreases the contribution $R_{v,11}$ of $u_e(t)$ to $P_{\rho,CL}^{-1}$ via the term $-R_{v,12} R_{v,22}^{-1} R_{v,12}^T$. Consequently, the precision $P_{\rho,CL}^{-1}$ is larger than $P_{\rho,OL}^{-1}$ when the spectrum of $u_r(t)$ (i.e. $|S_{id}(e^{j\omega})|^2 \Phi_r(\omega)$) is chosen equal to $\Phi_u^{OL}(\omega) \forall \omega$, but the converse holds when $\Phi_u^{CL}(\omega) = \Phi_{u_r}(\omega) + \Phi_{u_e}(\omega)$ is equal to $\Phi_u^{OL}(\omega) \forall \omega$.

The coupling between $\hat{\rho}_N$ and $\hat{\eta}_N$ is also the reason why $P_{\eta,OL} \leq P_{\eta,CL}$. Even though the coupling effect decreases for higher SNR (corresponding to large Ξ_{CL}), the coupling always has a negative effect on the performance of closed-loop identification for both the plant and the noise model. Indeed, if the coupling matrix $R_{v,12}$ were equal to 0, one would have $P_{\eta,CL} = P_{\eta,OL} = R_{v,22}$ and the contribution of $u_e(t)$ to $P_{\rho,CL}^{-1}$ would be maximized: $P_{\rho,CL}^{-1} = \Xi_{CL} + R_{v,11}$. A trivial case where the coupling between $\hat{\rho}_N$ and $\hat{\eta}_N$ is null is the case where no noise model parameters are identified. This is e.g. the case when the true system is in the Output Error form ($H(z, \eta_0) = 1$).

For $R_{v,12}$ to be 0 when the true system is really Box-Jenkins, we see that each element of the vector $C_{id}S_{id}\Lambda_\rho(z, \theta_0)$ should be orthogonal (as a function defined on the unit circle) to each element of the vector $\Lambda_\eta(z, \eta_0)/H(z, \eta_0)$. Consequently, for a given true system, it is the value of the controller C_{id} which will make the coupling $R_{v,12}$ important or not.

III. DESIGN OF CLOSED LOOPS WITH SATISFACTORY CLOSED-LOOP PERFORMANCE AND HIGH ACCURACY FOR IDENTIFICATION

A. General idea

The controller C_{id} which is present in the loop is generally determined in order to achieve good H_∞ performance with the true system and not to increase the accuracy of closed-loop identification in this loop. However, if one is about to design a controller C_{id} for a true system (1) and one knows that frequent re-identification of $G(z, \rho_0)$ and $H(z, \rho_0)$ will be necessary in the future e.g. for the purpose of performance monitoring, then, it could be worthwhile to add to the standard H_∞ performance objectives the additional objective of obtaining a controller for which $R_{v,12}$ is as close as possible to 0, or indeed equal to 0 (if possible). Thereby one would increase the accuracy of the subsequent closed-loop identifications. This section explains how this can be done.

B. Youla approach to deal with H_∞ constraints

Let us consider a stable BJ true system $\{G_0(z); H_0(z)\}$ (or in practice a model of this true system). We use a methodology which was used in the early ages of H_∞ control [17] to obtain a controller achieving the H_∞ specifications and that we modify to encompass the constraint of a matrix $R_{v,12}$ having the smallest norm possible. This method consists of designing C_{id} via its Youla parameter $Q(z)$ [16]. The set of all controllers C_{id} stabilizing the true system $G_0(z)$ is given by $C_{id} = \frac{Q}{1-QG_0}$ where $Q(z)$ is just constrained to be a stable transfer function. An important property of the Youla parametrization is that all closed-loop transfer functions are affine in $Q(z)$. In particular: $S_{id} = 1 - QG_0$ and $C_{id}S_{id} = Q$. In this paper, we will restrict the set of $Q(z)$ to the set of all FIR extensions of length M : $Q(z) = \sum_{i=0}^M q_i z^{-i}$ where q_i

($i = 0 \dots M$) are the parameters to be determined.

Due to the fact that all closed-loop transfer functions are affine in $Q(z)$, typical H_∞ constraints such as $|S_{id}(e^{j\omega})|^2 < |W_1(e^{j\omega})|^2 \forall \omega$ and $|C_{id}(e^{j\omega})S_{id}(e^{j\omega})|^2 < |W_2(e^{j\omega})|^2 \forall \omega$ can be easily formulated in this framework. Indeed, using the Schur complement [7][pp. 7-8], the constraint $|S_{id}(e^{j\omega})|^2 < |W_1(e^{j\omega})|^2 \forall \omega$ is seen to be equivalent to the following LMI:

$$\begin{pmatrix} |W_1(e^{j\omega})|^2 & 1 - \sum_{i=0}^M q_i G_0(e^{j\omega}) e^{-j i \omega} \\ (\cdot)^* & 1 \end{pmatrix} > 0 \quad \forall \omega \quad (18)$$

and the constraint $|C_{id}(e^{j\omega})S_{id}(e^{j\omega})|^2 < |W_2(e^{j\omega})|^2 \forall \omega$ is equivalent to the following LMI:

$$\begin{pmatrix} |W_2(e^{j\omega})|^2 & \sum_{i=0}^M q_i e^{-j i \omega} \\ (\cdot)^* & 1 \end{pmatrix} > 0 \quad \forall \omega \quad (19)$$

C. Constraints on the norm of $R_{v,12}$

The additional constraint on the norm of $R_{v,12}$ can be also treated in the Youla framework. Here we choose as norm for $R_{v,12}$ the largest singular value of $R_{v,12}$. Then, the square of this largest singular value is smaller than ε if and only if $R_{v,12}R_{v,12}^T < \varepsilon I$ or equivalently via the Schur complement again, if and only if:

$$\begin{pmatrix} \varepsilon I & R_{v,12} \\ R_{v,12}^T & I \end{pmatrix} > 0 \quad (20)$$

This constraint on $R_{v,12}$ can be transformed into an LMI in the decision variables q_i ($i = 0 \dots M$):

$$\begin{pmatrix} \varepsilon I & \sum_{i=0}^M q_i L_i \\ \sum_{i=0}^M q_i L_i & I \end{pmatrix} > 0 \quad (21)$$

where L_i ($i = 0 \dots M$) are known matrices of the dimension of $R_{v,12}$. The latter is possible because each entry of $R_{v,12}$ can be written as a linear combination of the decision variables q_i . Any entry r of $R_{v,12}$ can indeed be written as $r = \sum_{n=0}^{\infty} f(n)z(n)$ where $f(n)$ ($n = 0 \dots \infty$) is the impulse response of a particular entry of $C_{id}S_{id}\Lambda_\rho(z) = Q(z)\Lambda_\rho(z)$ and $z(n)$ the impulse response of a particular entry of $\Lambda_\eta(z)H_0^{-1}$. The impulse response $f(n)$ is a linear combination of the design parameters q_i ($i = 0 \dots M$): $f(n) = \sum_{i=0}^M q_i \lambda(n-i)$ where $\lambda(n)$ is the impulse response of the particular element of $\Lambda_\rho(z)$. This yields:

$$\begin{aligned} r &= \sum_{n=0}^{\infty} \sum_{i=0}^M q_i \lambda(n-i) z(n) \\ &= \sum_{i=0}^M q_i \underbrace{\left(\sum_{n=0}^{\infty} \lambda(n-i) z(n) \right)}_{\xi_i} \end{aligned}$$

where ξ_i ($i = 0 \dots M$) can be computed. The matrix L_i is then made up of the scalar ξ_i for each entry of $R_{v,12}$.

D. Algorithm

We now determine the optimal values for the parameters q_i ($i = 0 \dots M$) as those values for which the largest singular value of $R_{v,12}$ is minimized while guaranteeing the H_∞ constraints $|S_{id}(e^{j\omega})|^2 < |W_1(e^{j\omega})|^2 \forall \omega$ and $|C_{id}(e^{j\omega})S_{id}(e^{j\omega})|^2 < |W_2(e^{j\omega})|^2 \forall \omega$. Based on what has been deduced above, this can be done by solving the following LMI-based optimization problem:

$$\min_{q_i \ (i=0 \dots M)} \quad \varepsilon$$

subject to the LMI constraints (21), (18) and (19). We observe that the constraints (18) and (19) must be verified at each ω . This is impossible in practice. This problem can nevertheless be circumvented by using a finite frequency grid or by using the Kalman-Yakubovitch-Popov Lemma [15]. Once the optimal parameters q_i^{opt} ($i = 0 \dots M$) have been determined, the optimal controller C_{id} can thereafter be computed via: $C_{id} = \frac{Q^{opt}}{1 - Q^{opt}G_0}$ where $Q^{opt}(z) = \sum_{i=0}^M q_i^{opt} z^{-i}$. To sum up, the controller designed via this algorithm is guaranteed to achieve the required H_∞ performance, but has also been designed to allow accurate closed-loop identification. In Section V, a simulation example will be developed to illustrate the ideas of this section. In this simulation example, we will use a finite frequency grid for the LMI's (18) and (19).

Remark. As can be seen in (15) and in (17), the accuracy of the closed-loop identification is not only increased when $R_{v,12}$ is made small, but is also increased when Ξ_{CL} and $R_{v,11}$ are made large ($R_{v,22}$ cannot be influenced). As for $R_{v,12}$, the values of Ξ_{CL} and $R_{v,11}$ are also influenced by the choice of the controller C_{id} . However, forcing Ξ_{CL} and $R_{v,11}$ to be large would imply forcing the two-norm of S_{id} and $C_{id}S_{id}$ to be large. Consequently, unlike forcing $R_{v,12}$ to be small, forcing Ξ_{CL} and $R_{v,11}$ to be large would be in contradiction with closed-loop H_∞ performance specifications such as $|S_{id}(e^{j\omega})|^2 < |W_1(e^{j\omega})|^2 \forall \omega$ and $|C_{id}(e^{j\omega})S_{id}(e^{j\omega})|^2 < |W_2(e^{j\omega})|^2 \forall \omega$.

IV. OPEN-LOOP VS. CLOSED-LOOP: THE LEAST COSTLY IDENTIFICATION CONTEXT

We will now analyze the consequences of Proposition 1 in the context of a recently developed optimal experiment design framework: the least costly identification framework [5] (where the criteria for least cost need to be defined, and this is done below for two possibilities). This framework has as objective to identify, at the lowest economical cost, a model of the plant transfer function $G(z, \rho_0)$ with a minimal guaranteed precision i.e. a model for which

$$P_\rho^{-1} \geq R_{adm} \quad \text{or} \quad \text{var}(G(e^{j\omega}, \hat{\rho}_N)) \leq r_{adm}(\omega) \quad \forall \omega \quad (22)$$

where R_{adm} and $r_{adm}(\omega)$ are given and represent the required accuracy for the intended use of the model. In earlier

papers, it is shown how to compute the excitation signal and the duration N for the identification corresponding to the lowest economical cost under the constraint (22) and with a definition of cost as given below. This is shown for both an open-loop identification (see [6]) and for a closed-loop identification with a given controller in the loop (see [5]). Here, we address the question of knowing whether the cheapest cost will be obtained in open-loop identification or in closed-loop identification. We will see in the next two subsections that the lowest cost will be obtained alternatively by an open-loop identification and a closed-loop identification, depending on how the cost of the identification is defined.

A. Cost is defined via the power of $y_r(t)$

Suppose that the output $y(t)$ of a real-life system such as (1) must be kept around the set-point 0 (e.g. y is a quality measure of a product to be sold). This is done in closed loop with an available controller C_{id} (not necessarily designed as in Section III), but can also be done, if necessary, in open loop by forcing $u(t) = 0$. From the control and the production quality points of view, the closed-loop setup seems highly preferable since, for example, the controller allows one to reduce the effects of the disturbances on the output. However, the open-loop setup could be used for identification purposes if open-loop identification appeared optimal in some way.

In this situation of a production unit, the cost of the identification can be measured by the extra perturbation induced by the excitation signal on the output $y(t)$. For a closed-loop identification, this cost can be measured by \mathcal{P}_{y_r} , the power of the perturbation $y_r(t) = G_0 S_{id} r(t)$ due to the excitation signal $r(t)$ while, in open-loop identification, this cost can be measured by \mathcal{P}_{y_u} , the power of the perturbation $y_u(t) = G_0 u_{OL}(t)$ due to the excitation signal $u_{OL}(t)$:

$$\begin{aligned} \mathcal{P}_{y_r} &= \frac{1}{2\pi} \int_{-\pi}^{\pi} |G_0(e^{j\omega})S_{id}(e^{j\omega})|^2 \Phi_r(\omega) d\omega \\ \mathcal{P}_{y_u} &= \frac{1}{2\pi} \int_{-\pi}^{\pi} |G_0(e^{j\omega})|^2 \Phi_u^{OL}(\omega) d\omega \end{aligned} \quad (23)$$

In this section, we show that opening the loop to do the identification is in no way necessary since the closed-loop configuration is also the configuration which allows one to obtain a model of the plant $G(z, \rho_0)$ for which (22) holds with the least possible perturbation on the output of the process i.e. with the least possible economical cost:

Theorem 1: Consider the least costly experiment design problem consisting of obtaining, at the lowest economical cost, a model $G(z, \hat{\rho}_N)$ fulfilling (22) for some given R_{adm} and for some given identification duration N . The cost of an open-loop identification is defined by \mathcal{P}_{y_u} and the cost of the closed-loop identification is defined by \mathcal{P}_{y_r} (see (23)). Then, independently of the required accuracy R_{adm} and of the controller C_{id} present in the loop, (22) can always be obtained at a lower cost via closed-loop identification than via open-loop identification.

Proof. Denote by $\Psi(\omega)$ the spectrum $\Phi_u^{OL}(\omega)$ of the optimal open-loop identification i.e. the identification with the smallest \mathcal{P}_{y_u} while guaranteeing $P_{\rho,OL}^{-1} \geq R_{adm}$. Denote also by $\mathcal{C}_{opt,OL}$ the cost \mathcal{P}_{y_u} of this optimal open-loop experiment. Consider now the closed-loop experiment with $\Phi_r(\omega) = \frac{\Psi(\omega)}{|S_{id}(e^{j\omega})|^2}$. Note that the cost \mathcal{P}_{y_r} of this particular closed-loop experiment is equal to $\mathcal{C}_{opt,OL}$. Moreover, according to Proposition 1, this closed-loop experiment delivers a model $G(z, \hat{\rho}_N)$ for which:

$$P_{\rho,CL}^{-1} > P_{\rho,OL}^{-1} \geq R_{adm} \quad (24)$$

Consequently, the accuracy $P_{\rho,CL}^{-1}$ of this experiment is strictly superior to R_{adm} while having the same cost as the optimal open-loop identification. This implies by continuity that there exists a spectrum $\Phi_r(\omega)$ smaller than $\frac{\Psi(\omega)}{|S_{id}(e^{j\omega})|^2}$ and corresponding thus to a smaller cost \mathcal{P}_{y_r} than $\mathcal{C}_{opt,OL}$ which delivers a model for which $P_{\rho,CL}^{-1} \geq R_{adm}$. ■

In the considered situation, the open-loop setup is thus the less attractive from all points of view: there is no disturbance rejection **and** the perturbation induced by the identification excitation signal is larger than with closed-loop identification (see Theorem 1). Note that the result of this theorem is independent of the controller C_{id} present in the loop. However, obviously, if the controller present in the loop at the time of the identification has been designed as in Section III, the benefit of closed-loop identification with respect to open-loop identification will even be larger and this independently of the value of R_{adm} in (22). Note also that, if one is allowed to design the controller C_{id} in the loop at the moment where the closed-loop identification has to be performed and thus knowing the accuracy objective R_{adm} in (22), then the optimal controller to apply in the loop can be computed using the methods proposed in [11]. Note that the controller deduced with [11] is thus only optimal for closed-loop identification for the chosen value of R_{adm} in (22) and, unlike the algorithm presented in Section III, this controller is not guaranteed to achieve satisfactory closed-loop H_∞ performance (such as e.g. tracking and disturbance rejection).

As proven in e.g. [14], closed-loop identification with a minimum variance controller is optimal when the accuracy of the estimate has to be maximized and a constraint is posed on the maximal power of the total output $y(t) = y_r(t) + y_e(t)$ (see (3)). The illustration of Section V will show that the minimum variance controller is not optimal in the least costly identification experiment framework. Moreover, since, in a nutshell, the dynamics of this controller are similar to the inverse of the dynamics of the system, the minimum variance controller has very poor robustness. For these reasons, the preference should go to a classical H_∞ controller with (or without) the additional constraint (21).

Remark. Theorem 1 also holds when, for user-chosen constants α_y and α_u , the cost of the identification is defined as $\alpha_y \mathcal{P}_{y_r} + \alpha_u \mathcal{P}_{u_r}$ for closed-loop identification and as $\alpha_y \mathcal{P}_{y_u} + \alpha_u \mathcal{P}_u$ for open-loop identification. Here \mathcal{P}_{u_r} is the power of the signal $u_r(t)$ in (3) and \mathcal{P}_u is the power of the input signal $u(t)$. The case considered in Theorem 1 is the case $\alpha_y = 1$ and $\alpha_u = 0$.

B. Cost is defined by the duration N

The second situation also considers a true system (1) that has to be identified at the lowest cost in such a way that (22) holds. However, here, the economical cost of the identification is entirely determined by its duration N . Assuming that the identification can be performed either in open-loop or in closed loop, the objective of this section is to determine which identification conditions (i.e. open-loop or closed-loop) allows achievement of (22) with the smallest amount of data.

In both identification conditions, the number of data required to obtain the required accuracy can be reduced by increasing the power of the excitation signal. A physical limitation, though, to that increase is the limitations of the actuators. If we denote by $\Upsilon(\omega)$ the largest spectrum allowed by the actuators, the optimal open-loop input spectrum is therefore $\Phi_u^{OL}(\omega) = \Upsilon(\omega) \forall \omega$ and the optimal closed-loop excitation spectrum is the spectrum $\Phi_r(\omega)$ such that $\Phi_u^{CL}(\omega) = \Upsilon(\omega) \forall \omega$. Given this, the following theorem shows that open-loop identification is optimal in this context. Indeed, the optimal open-loop identification described above will need less data points to obtain (22) than the optimal closed-loop identification.

Theorem 2: Given a BJ true system (1), consider two identification experiments, one in open loop and one in closed-loop with a controller C_{id} in the loop. Suppose furthermore that these identification experiments are such that $\Phi_u^{OL}(\omega) = \Phi_u^{CL}(\omega) = \Upsilon(\omega) \forall \omega$. Then, the minimal number of data required to obtain $P_\rho^{-1} \geq R_{adm}$ for any given R_{adm} is smaller in open-loop than in closed-loop identification except when $R_{v,12}$ in (10) is equal to 0 in which case this number of data is the same for both identification conditions.

Proof. The result for $R_{v,12} \neq 0$ is a direct consequence of Proposition 1 (Item 2). Indeed, for each value of N , the open-loop identification considered here gives an accuracy which is larger than the considered closed-loop identification: $P_{\rho,OL}^{-1} \geq P_{\rho,CL}^{-1}$. Since both $P_{\rho,OL}^{-1}$ and $P_{\rho,CL}^{-1}$ are proportional to N , the required accuracy R_{adm} will be attained with a smaller N in open loop than in closed loop. The result when $R_{v,12} = 0$ is a consequence of the fact that, in this case, $P_{\rho,OL}^{-1} = P_{\rho,CL}^{-1}$ for each value of N . ■

This result in the least costly context is very close to the result in classical optimal experiment design that states that

open-loop identification is optimal when the power of the input is constrained. Variants of this result can be found in [14], [13][Chapter 13] and [1]. The proof of Theorem 2 is very close to the proof in [1].

V. SIMULATION RESULTS

In order to illustrate the results of this paper, we consider the following first-order true system:

$$S: y(t) = \frac{b_0 z^{-1}}{1 + f_0 z^{-1}} u(t) + \frac{1 + c_0 z^{-1}}{1 + d_0 z^{-1}} e(t) \quad (25)$$

with $b_0 = 0.36$, $f_0 = -0.7$, $c_0 = 0.6$, $d_0 = 0.1$ and $\sigma_e^2 = 1$. We compare the variance results of open-loop and direct closed-loop identification on that true system. For the closed-loop experiment, we will consider different controllers C_{id} in the loop: the first controller $C_{id,1}$ is an H_∞ controller achieving the following H_∞ performance: $|S_{id}(e^{j\omega})| < |W_1(e^{j\omega})| \forall \omega$ and $|C_{id}S_{id}(e^{j\omega})| < |W_2(e^{j\omega})| \forall \omega$ with

$$W_1(z) = \frac{2.525z^2 - 5z + 2.475}{z^2 - z + 0.25} \quad (26)$$

$$W_2(z) = \frac{2.604z^2 - 1.042z + 0.1042}{z^2 - 1.333z + 0.4444}$$

These weightings are represented in Figures 1 and 2 and guarantee that the controller has some roll-off, that the bandwidth of the closed-loop is about 0.5 rad/s , that the low-frequency disturbances are reduced with 60 dB , and that the resonance peaks of the the transfer functions S_{id} and $C_{id}S_{id}$ are limited to $\pm 6 \text{ dB}$. The second and third controllers we will test ($C_{id,2}$ and $C_{id,3}$) are controllers having the same performance specifications as the first one, but for which the norm of $R_{v,12}$ is minimized (see Section III). For the second controller, we choose the length M of the expansion of the Youla parameter equal to 15 and for the third controller $M = 6$. As an illustration, in Figures 1 and 2, the modulus of the sensitivity function S_{id} and the transfer functions $C_{id}S_{id}$ corresponding to the controller $C_{id,3}$ are compared with the modulus of the weighting functions W_1 and W_2 , respectively. Finally, the fourth controller $C_{id,4}$ is the minimum variance controller for (25).

To illustrate (some of) the results of Proposition 1, we compute the covariance matrices for $\hat{\rho}_N$ and $\hat{\eta}_N$ using the formulae (14)-(17) when $\Phi_u^{OL}(\omega)$ is the spectrum of a white noise of variance 1 for the open-loop identification and when $|S_{id}(e^{j\omega})|^2 \Phi_r(\omega) = \Phi_u^{OL}(\omega) \forall \omega$ for the closed-loop identification. The results obtained for open-loop identification and for closed-loop identifications with the four different controllers are compared in Figures 3 and 4. In these figures, we compare the 95%-confidence region for $\hat{\rho}_N - \rho_0$ and $\hat{\eta}_N - \eta_0$, obtained in the five different cases. These uncertainty regions are $U_\rho = \{\Delta\rho \mid \Delta\rho^T P_\rho^{-1} \Delta\rho \leq 5.99\}$ and $U_\eta = \{\Delta\eta \mid \Delta\eta^T P_\eta^{-1} \Delta\eta \leq 5.99\}$, respectively.

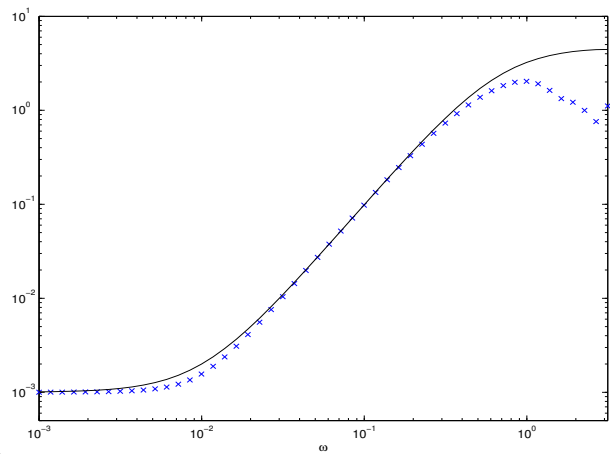


Fig. 1. Modulus of the the sensitivity function S_{id} corresponding to the controllers $C_{id,3}$ (blue crosses) compared to the modulus of $W_1(e^{j\omega})$ (black solid).

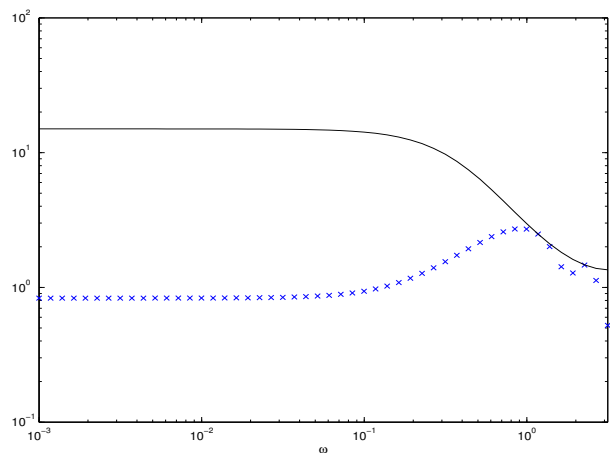


Fig. 2. modulus of the transfer functions $C_{id}S_{id}$ corresponding to the controllers $C_{id,3}$ (blue crosses) compared to the modulus of $W_2(e^{j\omega})$ (black solid).

The figures confirm the results Proposition 1 (Items 1 and 3). Indeed, we see in Figure 3 that, for each of the four controllers, $P_{\rho,OL} > P_{\rho,CL}$ and thus $U_{\rho,OL} \supset U_{\rho,CL}$. In Figure 4, we see that, for each of the four controllers, $P_{\eta,OL} < P_{\eta,CL}$ and thus that $U_{\eta,OL} \subset U_{\eta,CL}$. We see that the controller $C_{id,2}$ which guarantees the H_∞ specifications while minimizing the norm of $R_{v,12}$ has, as expected, the best results for both uncertainty regions. Indeed, due to the relatively long Youla parameter ($M = 15$), it was possible to obtain a norm of $R_{v,12}$ as small as 0.05. This allows to obtain $P_{\eta,OL} \approx P_{\eta,CL}$ and thus $U_{\eta,OL} \approx U_{\eta,CL}$ and a relatively small $P_{\rho,CL}$ and $U_{\rho,CL}$ with respect to the other controllers. The result with controller $C_{id,3}$ are very nice too even if the complexity is reduced to $M = 6$. Finally, we see that the three H_∞ controllers (i.e. with or without the additional constraint on the norm of $R_{v,12}$) give much smaller uncertainties than the minimum variance controller $C_{id,4}$.

Now, let us proceed to least costly identification experiment design and more particularly the situation presented in Section IV-A. We have computed using the techniques of [5] the minimal cost \mathcal{P}_{y_u} in open-loop and \mathcal{P}_{y_r} in closed-loop for which the largest relative error between $G(z, \hat{\rho}_N)$ and $G(z, \rho_0)$ is guaranteed to be smaller than 0.2 at each frequency. The corresponding minimal costs are given in Table V. These results confirms Theorem 1 and what was observed in Figure 3.

$\mathcal{P}_{y_u}^{opt}$	1.10
$\mathcal{P}_{y_r}^{opt}$ for $C_{id,1}$	0.87
$\mathcal{P}_{y_r}^{opt}$ for $C_{id,2}$	0.55
$\mathcal{P}_{y_r}^{opt}$ for $C_{id,3}$	0.75
$\mathcal{P}_{y_r}^{opt}$ for $C_{id,4}$	1.07

TABLE I

RESULTS OF THE LEAST COSTLY EXPERIMENT DESIGN

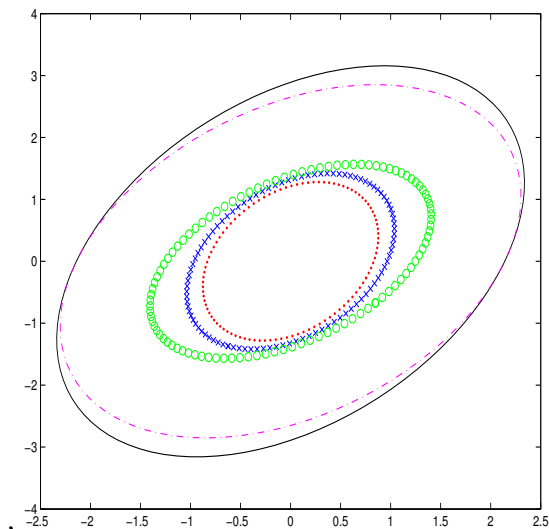


Fig. 3. U_ρ in open-loop identification (black solid), in closed-loop identification with $C_{id,1}$ (green circles), $C_{id,2}$ (red dotted), $C_{id,3}$ (blue crosses) and $C_{id,4}$ (magenta dashdot). Figure scaled for $N = 1$

VI. CONCLUSIONS

In this paper, we develop an algorithm to determine a controller which both achieve good H_∞ performance with the true system and ensures that the accuracy of a closed-loop identification on the designed loop is high. Moreover, we analyze whether open-loop or closed-loop identification is optimal in the least costly identification experiment design framework.

REFERENCES

[1] J. C. Aguero and G. Goodwin. On the optimality of open and closed loop experiments in system system identification. In *CD-ROM Proc. 45th Conference on Decision and Control, San Diego*, 2006.

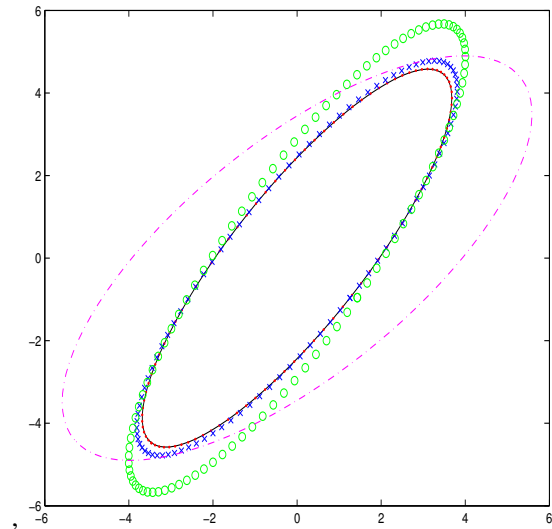


Fig. 4. Same as Figure 1 but for U_η . The ellipses corresponding to open-loop identification (black solid) and closed-loop identification with $C_{id,2}$ (red dotted) overlap.

- [2] M. Barenthin, H. Jansson, and H. Hjalmarsson. Applications of mixed H_2 and H_{inf} input design in identification. In *Proc. IFAC World Congress, Prague*, 2005.
- [3] X. Bombois, M. Gevers, and G. Scorletti. Open-loop versus closed-loop identification of Box-Jenkins models: a new variance analysis. In *CD-ROM Proc. 44th Conference on Decision and Control, Seville*, 2005.
- [4] X. Bombois, M. Gevers, G. Scorletti, and B.D.O. Anderson. Robustness analysis tools for an uncertainty set obtained by prediction error identification. *Automatica*, 37(10):1629–1636, 2001.
- [5] X. Bombois, G. Scorletti, M. Gevers, P. Van den Hof, and R. Hildebrand. Least costly identification experiment for control. *Automatica*, 42(10):1651–1662, 2006.
- [6] X. Bombois, G. Scorletti, M. Gevers, R. Hildebrand, and P. Van den Hof. Cheapest open-loop identification for control. In *CD-ROM Proc. 43th Conference on Decision and Control, Bahamas*, 2004.
- [7] S. Boyd, L. El Ghaoui, E. Feron, and V. Balakrishnan. *Linear Matrix Inequalities in Systems and Control Theory*, volume 15 of *Studies in Appl. Math.* SIAM, Philadelphia, June 1994.
- [8] U. Forssell and L. Ljung. Closed-loop identification revisited. *Automatica*, 35:1215–1241, 1999.
- [9] M. Gevers and L. Ljung. Optimal experiment design with respect to the intended model applications. *Automatica*, 22:543–554, 1986.
- [10] H. Hjalmarsson, M. Gevers, and F. De Bruyne. For model-based control design, closed-loop identification gives better performance. *Automatica*, 32(12):1659–1673, 1996.
- [11] H. Hjalmarsson and H. Jansson. Closed-loop experiment design for linear dynamical systems via LMI's. Submitted to *Automatica*, 2006. Short version presented at the IFAC World Congress 2005.
- [12] H. Jansson and H. Hjalmarsson. Mixed H_∞ and H_2 input design for identification. In *Proc. 43th IEEE Conference on Decision and Control, The Bahamas*, pages 388–393, 2004.
- [13] L. Ljung. *System Identification: Theory for the User, 2nd Edition*. Prentice-Hall, Englewood Cliffs, NJ, 1999.
- [14] T.S. Ng, G.C. Goodwin, and T. Soderstrom. Optimal experiment design for linear systems with input-output constraints. *Automatica*, 13(6):571–577, 1977.
- [15] V.M. Popov. *Hyperstability of Control Systems*. Springer-Verlag, New-York, 1973.
- [16] M. Vidyasagar. *Control System Synthesis: a factorization approach*. MIT Press, Cambridge, Mass, 1985.
- [17] G. Zames. Feedback and optimal sensitivity: Model reference transformations, multiplicative seminorms, and approximate inverses. *IEEE Trans. Aut. Control*, AC-26(2):301–320, April 1981.
- [18] K. Zhou and J. Doyle. *Essentials of Robust Control*. Prentice Hall, Upper Saddle River, New Jersey, 1998.